Analytical and Bioanalytical Chemistry (2020) 412:5653–5661
https://doi.org/10.1007/s00216-020-02785-4

RESEARCH PAPER

Highly sensitive and selective detection of 4-nitroaniline in water by a novel fluorescent sensor based on molecularly imprinted poly(ionic liquid)

Wei Xie[1,2] · Jian Zhang[2] · Yanbo Zeng[2] · Hailong Wang[2] · Yiwen Yang[2] · Yunyun Zhai[2] · Dongwei Miao[1] · Lei Li[2]

Received: 6 January 2020 / Revised: 12 June 2020 / Accepted: 22 June 2020 / Published online: 3 July 2020

Abstract

A novel molecularly imprinted fluorescent sensor for the determination of 4-nitroaniline (4-NA) was synthesized via free radical polymerization with 3-[(7-methoxy-2-oxo-2*H*-chromen-4-yl)methyl]-1-vinyl-1*H*-imidazol-3-ium bromide as the fluorescence functional monomer, 4-NA as the template molecule, ethylene glycol dimethacrylate as the cross-linker, and 2,2′-azo(bisisobutyronitrile) as the initiator. The obtained fluorescent poly(ionic liquid) was characterized through Fourier transform infrared, scanning electron microscopy, Brunauer–Emmett–Teller analysis, and fluorescence spectrophotometry. The fluorescent sensor had high fluorescence intensity, short detection time (0.5 min), good selectivity, and excellent sensitivity (limit of detection = 0.8 nM) for 4-NA, with good linear relationships of 2.67–10,000 nM. The practical applicability of the fluorescence sensor in detecting 4-NA in industrial wastewater and spiked environmental water was demonstrated, and a satisfactory result was obtained.

Keywords Fluorescent sensor · Molecular imprinting · Poly(ionic liquid) · 4-Nitroaniline

Introduction

4-Nitroaniline (4-NA) is an important chemical intermediate that is widely used in dyes, pesticides, pharmaceutical products, explosives, and rubber. In industrial production, 4-NA can be released into the environment in the form of industrial waste. Given that 4-NA has good solubility in water, it can easily penetrate and accumulate in soil or groundwater. 4-NA is highly toxic, mutagenic, and carcinogenic. It is not only highly toxic to aquatic organisms but also harmful to human health because it can lead to respiratory arrest, methemoglobinemia, liver injury, skin eczema, diarrhea, and anemia [1, 2]. 4-NA can cause long-term damage to the environment due to its poor biodegradability, high chemical stability, and persistence. Consequently, environmental protection agencies in many countries consider it a priority pollutant [3]. Therefore, establishing rapid, sensitive, selective methods for determining 4-NA is important.

At present, the main detection methods of 4-NA include spectrophotometry [4, 5], surface-enhanced Raman spectroscopy [6, 7], electrochemical method [8–10], fluorescence method [11, 12], high-performance liquid chromatography [13, 14], luminescence method [15, 16], and electrophoresis [17]. Chromatographic method (such as high-performance liquid chromatography) has the advantages of good separation effect and high sensitivity. And now, some aromatic amine samples (such as those in textiles or food contact materials) are still detected by chromatography-based methods [18–21]. However, due to the complex matrix of the sample or the low concentration of the analyte, some samples need to go through complicated pretreatment process before detection, which is complicated in operation and high in cost. Fluorescence method is an effective approach for the rapid detection of 4-NA because of its low detection limit, high sensitivity, rapidity, and use of simple instruments.

Electronic supplementary material The online version of this article (https://doi.org/10.1007/s00216-020-02785-4) contains supplementary material, which is available to authorized users.

✉ Yiwen Yang
yangyiwen@mail.zjxu.edu.cn

✉ Lei Li
lei.li@mail.zjxu.edu.cn

[1] School of Petrochemical Engineering, Changzhou University, Changzhou 213016, Jiangsu, China

[2] College of Biological, Chemical Sciences and Engineering, Jiaxing University, 118 Jiahang Road, Jiaxing 314001, Zhejiang, China

However, this method has shortcomings, such as unsatisfactory selectivity for target molecules, which leads to the interference of similar substances during determination.

Molecular imprinting is a new molecular recognition technology [22]. Its principle is to imitate the natural antigen–antibody reaction mechanism. The target molecule is used as the template molecule, and the functional monomer and cross-linking agent are polymerized under the action of the initiator. After polymerization, the target molecule is fixed in the polymer. After the target molecule is removed, the hole of the target molecule is left on the polymer material. The structure of the hole complements the size and shape of the target molecule. Hence, the hole has highly specific recognition and adsorption properties for target molecules.

Fluorescence assay has a low detection limit, high sensitivity, rapidity, and simple instrumentation. By combining it with molecular imprinting technology, a reliable, fast, highly specific, and sensitive analytical method may be developed for the accurate and efficient detection of 4-NA in water. The assay can overcome the shortcomings of traditional methods, such as low sensitivity, poor selectivity, complicated operation, and time-consuming sample pretreatment.

Recently, molecularly imprinted fluorescent polymers have made some progress in improving the selectivity of target molecules [23]. However, there are still some problems to be solved, such as the single type of phosphors and the poor water solubility of polymers.

Ionic liquid is a kind of liquid ionic compound at or near room temperature, in which there are only anions and cations and no neutral molecules [24]. Therefore, various ionic liquids can be synthesized through the design of anion and anion. The organic fluorescent functional group can be connected to the anion or cation structure of the alkenyl ionic liquid to prepare the alkenyl fluorescent ionic liquid, and then through the polymerization reaction, the fluorescent poly(ionic liquid) can be obtained. Because of the ionic liquid structure in the polymer, the water solubility of the polymer can be increased. It is beneficial to detect the target molecules in water samples.

In this study, we combined high-sensitivity fluorescence method with high-selectivity molecular imprinting technology and synthesized a novel molecular imprinting poly(ionic liquid) fluorescent sensor by using vinyl fluorescent ionic liquid as a monomer. We developed a new detection technology for environmental water samples and applied it to recognize and determine 4-NA in industrial wastewater and environmental water.

Experimental section

Materials

4-Bromomethyl-7-methoxycoumarin and 1-vinylimidazole were obtained from Tokyo Chemical Industry Co., Ltd. (Shanghai, China). Ethylene glycol dimethacrylate (EGDMA), 4-NA, 3-NA, and 2-NA were supplied by Sigma-Aldrich (Shanghai, China). 2,2′-Azo(bisisobutyronitrile) (AIBN), *p*-chloroaniline, diphenylamine, 4,4′-diaminobiphenyl, *p*-anisidine, *m*-toluidine, 4-nitrobenzyl bromide, and nitrobenzene were obtained from Aladdin (Shanghai, China). In addition, several common chemicals, including methanol, ethanol, trichloromethane, sodium dihydrogen phosphate, and sodium phosphate dibasic, were purchased from Sinopharm Chemical Reagent Co., Ltd. (Shanghai, China). Different pH phosphate buffers were prepared by mixing different volumes of 0.01 M NaH_2PO_4 and 0.01 M Na_2HPO_4. All chemicals and solvents were of pure analytical grade. Water was purified through a Milli-Q purification system and applied to the entire experimental process.

Apparatus

A Varian 400-MR nuclear magnetic resonance instrument (Varian, USA) was used to record ^{1}HNMR and ^{13}CNMR spectra. Fourier transform infrared (FT-IR) measurements were performed with a Nicolet Nexus-470 FT-IR apparatus. An F-7000 fluorescence spectrofluorometer (Hitachi, Japan) was utilized to obtain the fluorescence spectra. The fluorescence intensity was detected at excitation and emission wavelengths of 329 and 395 nm, respectively. N_2 adsorption–desorption isotherms were measured with Micro Tristar 2020 after all of the samples were degassed at 100 °C for 24 h. Brunauer–Emmett–Teller and Barrett–Joyner–Halenda methods were used to calculate the specific surface area and pore size distribution, respectively. The surface morphologies of all samples were analyzed with a Hitachi S-4800 scanning electron microscope (Hitachi, Japan). The samples of industrial wastewater were detected by Agilent 1260 high-performance liquid chromatography (HPLC).

Synthesis of ionic liquid functional monomer

A mixture of 4-bromomethyl-7-methoxycoumarin (2 mmol), 1-vinylimidazole (4 mmol), and trichloromethane (15 mL) was stirred in a 100-mL, round-bottom flask at 80 °C for 12 h. After the reaction was completed, the solvent trichloromethane was evaporated in a vacuum. The residue was washed with anhydrous ether. Then, the expected product, 3-((7-methoxy-2-oxo-2*H*-chromen-4-yl)methyl)-1-vinyl-1*H*-imidazol-3-ium bromide, was collected and further dried in a vacuum oven overnight (see Electronic Supplementary Material (ESM) Scheme S1).

Preparation of molecularly imprinted poly(ionic liquid) and non-imprinted poly(ionic liquid)

The reaction was carried out in a methanol solution using 4-NA as the template molecule, 3-((7-methoxy-2-oxo-2*H*-chromen-4-yl)methyl)-1-vinyl-1*H*-imidazol-3-ium bromide as the functional monomer, and EGDMA and AIBN as the cross-linker and initiator, respectively. The specific experimental process of synthesizing the molecularly imprinted poly(ionic liquid) (MIPIL) was as follows: 4-NA (0.1 mmol) and 3-((7-methoxy-2-oxo-2*H*-chromen-4-yl)methyl)-1-vinyl-1*H*-imidazol-3-ium bromide (0.4 mmol) were thoroughly dispersed in a methanol solution (40 mL) for 15 min in a 100-mL, round-bottom flask. Then, EGDMA (2 mmol) and AIBN (50 mg) were separately added to the reaction solution. After purging with nitrogen for 30 min, the round-bottom flask was sealed, and the mixture in it was stirred at 60 °C for 24 h. After the reaction was completed, polymerization products were obtained and collected via filtration. The desired products were completely washed with ethanol to remove 4-NA and dried at 80 °C in a vacuum oven overnight. Non-imprinted poly(ionic liquid) (NIPIL) was synthesized under the same conditions in the absence of 4-NA.

Fluorescence measurement

To obtain the best test conditions, we used 4-NA as the detection target, and its level was 1 μM. The levels of MIPIL ranging from 10 to 50 mg/L and the pH values of the solution from 4 to 11 (prepared by phosphate buffer solution) were optimized. Real-time detection of fluorescence intensity was performed every 10 s to obtain the stabilization time and determine the optimum detection time.

Determination of 4-NA in real samples

Industrial wastewater was supplied by a chemical factory in Jiangsu Province (China). Actual environmental water samples were obtained from Beijing–Hangzhou Grand Canal in Jiaxing City (Jiaxing, China). The suspended particles in the water samples were removed with a 0.45-μm filter, and then the actual water samples were directly used for detection.

Results and discussion

Characterization of ionic liquid functional monomer

In order to further determine the molecular structure of the prepared fluorescent functional monomer (3-((7-methoxy-2-oxo-2*H*-chromen-4-yl)methyl)-1-vinyl-1*H*-imidazol-3-ium bromide), we characterized the compound by NMR, and the results are shown in Fig. S1 (see ESM). Its NMR data were as follows:

- ^{1}HNMR (400 MHz, CD_3OD): $\delta = 9.52$ (s, 1H), 8.15 (s, 1H), 7.90 (s, 1H), 7.72 (d, $J = 9.2$ Hz, 1H), 7.31 (q, $J = 8.0$ Hz, 1H), 7.00 (dd, $J = 2.4$, 8.8 Hz, 1H), 6.94 (d, $J = 2.4$ Hz, 1H), 5.99 (dd, $J = 2.4$, 15.6 Hz, 1H), 5.95 (s, 1H), 5.84 (s, 2H), 5.50 (dd, $J = 2.4$, 8.8 Hz, 1H), and 3.90 (s, 3H)
- ^{13}CNMR (100 MHz, CD_3OD): $\delta = 163.7$, 160.7, 155.5, 148.5, 128.4, 124.8, 123.8, 123.8, 119.9, 112.7, 110.4, 110.1, 109.2, 100.9, 55.2, and 49.3

The above data showed that the functional monomers had been synthesized successfully.

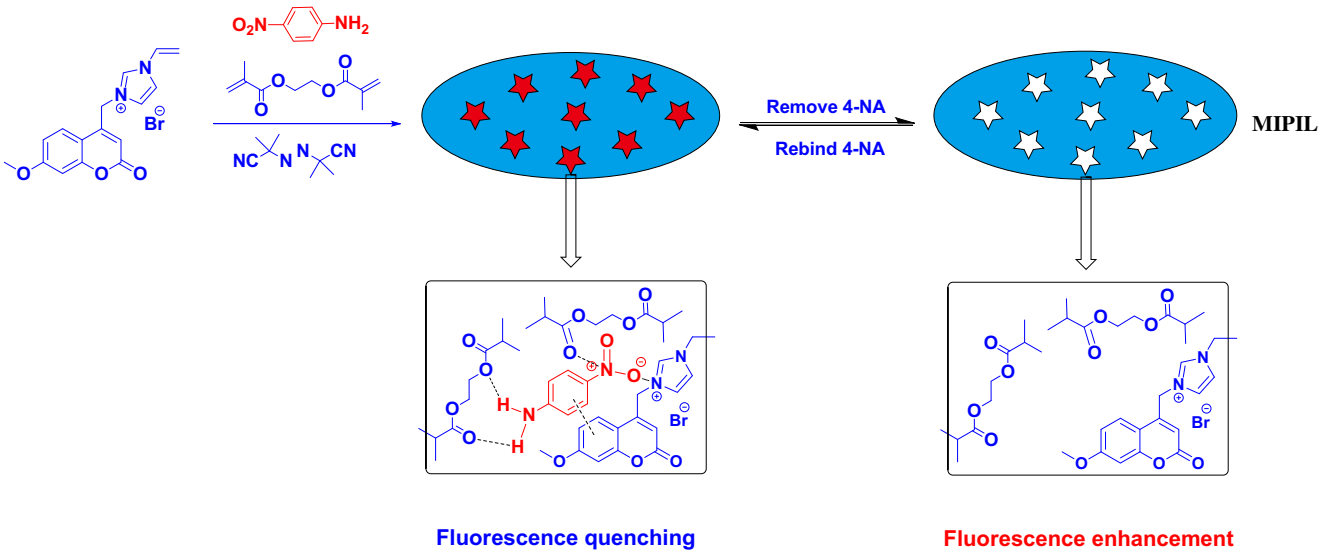

Scheme 1 Schematic of 4-NA determination

Preparation of MIPIL and NIPIL and the detection principle of 4-NA

The synthetic process of MIPIL and NIPIL was as follows: First, the fluorescent ionic liquid functional monomer (ILFM) was synthesized by introducing an electron-rich alkenyl imidazole group into 4-bromomethyl-7-methoxycoumarin to enhance the fluorescence intensity of the parent compound significantly, and second, polymerization was performed in the presence of AIBN as the initiator. During polymerization, 4-NA molecules were captured via ILFM and EGDMA through electrostatic attraction and hydrogen bonding, respectively. Fluorescence quenching of ILFM occurred due to the electron-deficient structure of 4-NA and its π–π stacking with ILFM. Lastly, 4-NA molecules were removed with an ethanol solution after polymerization, and the fluorescence of MIPIL was restored (Scheme 1).

Characterization of MIPIL and NIPIL

The structural properties of ILFM, MIPIL, and NIPIL were further analyzed using FT-IR spectra. Figure S2 (see ESM) showed that the characteristic peaks at 1732, 1637, and 1158 cm^{-1} were attributed to the stretching of C=O and C–O of EGDMA and ILFM, respectively. The typical peaks at 1560 and 1179 cm^{-1} represented the imidazolium cationic group vibrations of C=N, C=C, and C–N. The FT-IR spectra of NIPIL were almost similar to those of MIPIL. The analysis of the composition and structure of MIPIL or NIPIL via FT-IR spectra confirmed the successful polymerization of the ILFM and EGDMA cross-linker.

The scanning electron microscopy (SEM) image showed that MIPIL had an obvious structure with a clear outline, whereas the image of NIPIL was vague (Fig. 1). Moreover, MIPIL was more uniform than NIPIL in terms of size and shape. Figure 2a and c show that the nitrogen adsorption–desorption isotherms of MIPIL and NIPIL had the characteristics of type I and IV composite isotherms according to IUPAC classification [25]. In the low-pressure region ($P/P_0 < 0.1$), the adsorption amount of nitrogen increased rapidly, indicating that there were some micropores on the surfaces of both polymers. However, in the pressure zone ($0.1 < P/P_0 < 0.8$), the adsorption capacity of nitrogen increased slowly, and the rising speed of MIPIL was higher than that of NIPIL. After reaching the high-pressure region ($P/P_0 > 0.8$), the adsorption capacity of nitrogen increased rapidly, indicating that there were not only a certain amount of mesopores, but also a small number of macropores on the surface of the two polymers [26]. Both isotherms had H3-type hysteresis loops, indicating that both polymers had lamellar structures, with slit-like pore structures [27]. It was consistent with their SEM images (Fig. 1). The pore size distribution of MIPIL was mainly at 1.48 and 2.52 nm, while that of NIPIL was mainly at 1.18, 1.36, and 1.72 nm. The surface area of MIPIL and NIPIL was 20.14 and 18.60 m^2/g, respectively, and their average pore sizes were 12.36 and 11.60 nm, respectively (Fig. 2). The test result showed that MIPIL had a larger surface area and pore size than NIPIL. It indicated that MIPIL had some molecularly imprinted holes on its surface.

Optimization of 4-NA determination

To obtain the best detection effect, we optimized the detection conditions of MIPIL for detecting 4-NA. The adding concentration of MIPIL ranging from 10 to 50 mg/L was explored to investigate its effect on 4-NA detection. The results showed that the maximum fluorescence quenching efficiency was obtained when the MIPIL concentration was 30 mg/L (see ESM Fig. S3A). Therefore, the optimized level of 30 mg/L was selected as the best detection amount of MIPIL.

On the basis of this condition, real-time fluorescence monitoring of the mixture was performed to obtain the stability of the kinetic binding of MIPIL toward the 4-NA template molecules. As shown in Fig. S3C (see ESM), the fluorescence quenching equilibrium can be quickly achieved within 0.5 min at room temperature when the concentrations of 4-NA were 100 nM and 1 μM. In addition, the fluorescent signal could remain relatively stable for a long time. This

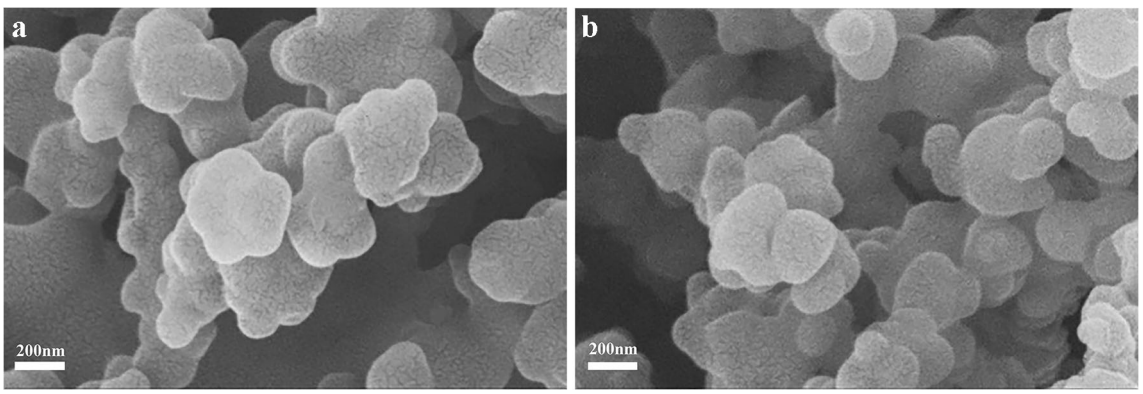

Fig. 1 SEM images of MIPIL (**a**) and NIPIL (**b**)

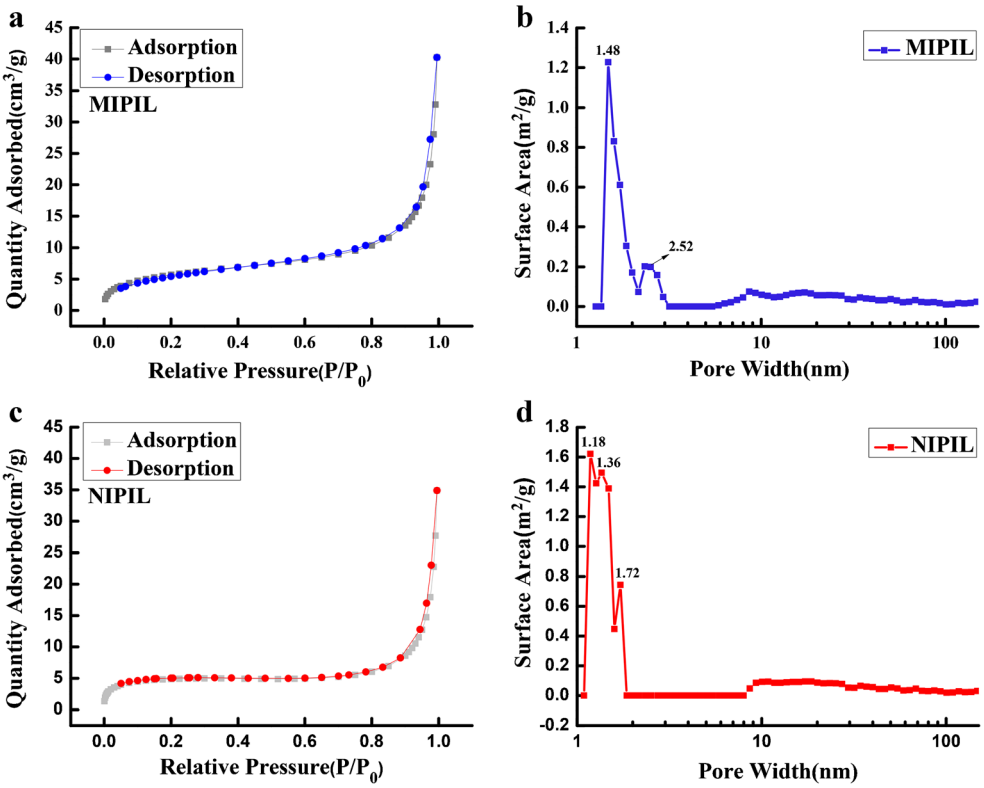

Fig. 2 N_2 adsorption–desorption isotherm and pore width distribution of MIPIL (**a**, **b**) and NIPIL (**c**, **d**)

phenomenon fully demonstrates that the 4-NA template molecules could rapidly match the binding sites in the space cavity to achieve the effect of fluorescence quenching. We conclude that the MIPIL fluorescence sensor can detect 4-NA rapidly and efficiently. The effect of the pH value ranging from 4 to 11 (prepared by phosphate buffer solution) on detection performance was also studied. The pH value of the solution had no significant effect on the detection of 4-NA (see ESM Fig. S3B). Given that the pH value of the water used in the experiment was 7, we set the best pH value of the detection system to 7.

Under these optimal conditions, different levels of 4-NA were tested using the MIPIL sensor. As shown in Fig. 3a, the fluorescence intensity of the sensor declined as the level of 4-NA increased. Figure 3b indicates that a good linear relationship exists between F_0/F and the 4-NA level in the concentration range of 2.67–10,000 nM. The linear equation is $F_0/F = 1.041 + 0.321C_{4\text{-NA}}$, and the correlation coefficient is 0.992. The limit of detection (LOD) was 0.8 nM (0.11 μg/L) (S/N = 3), and the limit of quantification (LOQ) was 0.37 μg/L (2.67 nM) (S/N = 10). Table 1 indicates that the assay has higher sensitivity for 4-NA compared with the majority of previously reported methods.

Selectivity of NIPIL and MIPIL sensors

The selective recognition capability of NIPIL and MIPIL fluorescence sensors was demonstrated by comparing it with that of 4-NA and its analog. Its analogs include (1) *p*-chloroaniline, (2) diphenylamine, (3) 4,4′-diaminobiphenyl,

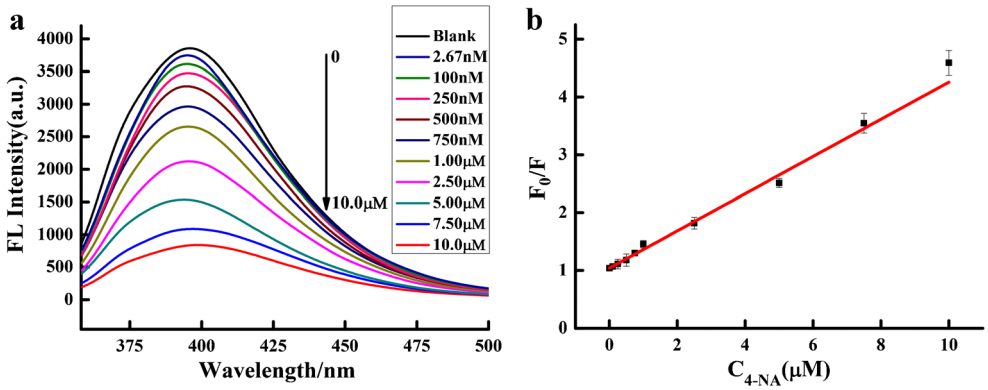

Fig. 3 Fluorescence spectra of MIPIL with the addition of different levels of 4-NA (**a**) and fluorescence quenching intensity of MIPIL in the presence of 4-NA with different levels (2.67–10,000 nM) (**b**). $\lambda_{ex} = 329$ nm and $\lambda_{em} = 395$ nm

Table 1 Comparison of the assay with other methods of detecting 4-NA

No.	Method	LOD (nM)	References
1	CSSNPs/CPE[a]	5	[8]
2	PBPMCz[b]	1100	[11]
3	CB[6]@QDs[c]	60	[12]
4	Ag@MIP[d]	0.001	[7]
5	Copper nanoparticle-embedded chitosan	370	[9]
6	CS@CPE[e]	93.4	[10]
7	Silver particles on graphite electrode	41.8	[28]
8	1,2,3-Triazolyl-based conjugated microporous polymer	4200	[29]
9	Molecularly imprinted polymeric ionic liquid	9	[30]
10	Triphenylamine-functionalized luminescent sensor	725 (0.1 ppm)	[31]
11	3D metal–organic frameworks	637 (88 ppb)	[32]
12	Binder-free chemical sensor electrodes	500	[2]
13	Cd(II) metal–organic framework	4930 (0.88 ppm)	[33]
14	Silver electrode	4.74	[34]
15	MIPIL sensor	0.8	This work

[a] Chitosan-stabilized silver nanoparticles on the carbon paste electrode

[b] Ketone-functionalized carbazolic porous framework

[c] Cucurbit[6]uril-modified CdTe quantum dot fluorescent probe

[d] Core–shell Ag@molecularly imprinting polymer

[e] Carbon paste electrode modified with a chitosan solution gelled in acetic acid

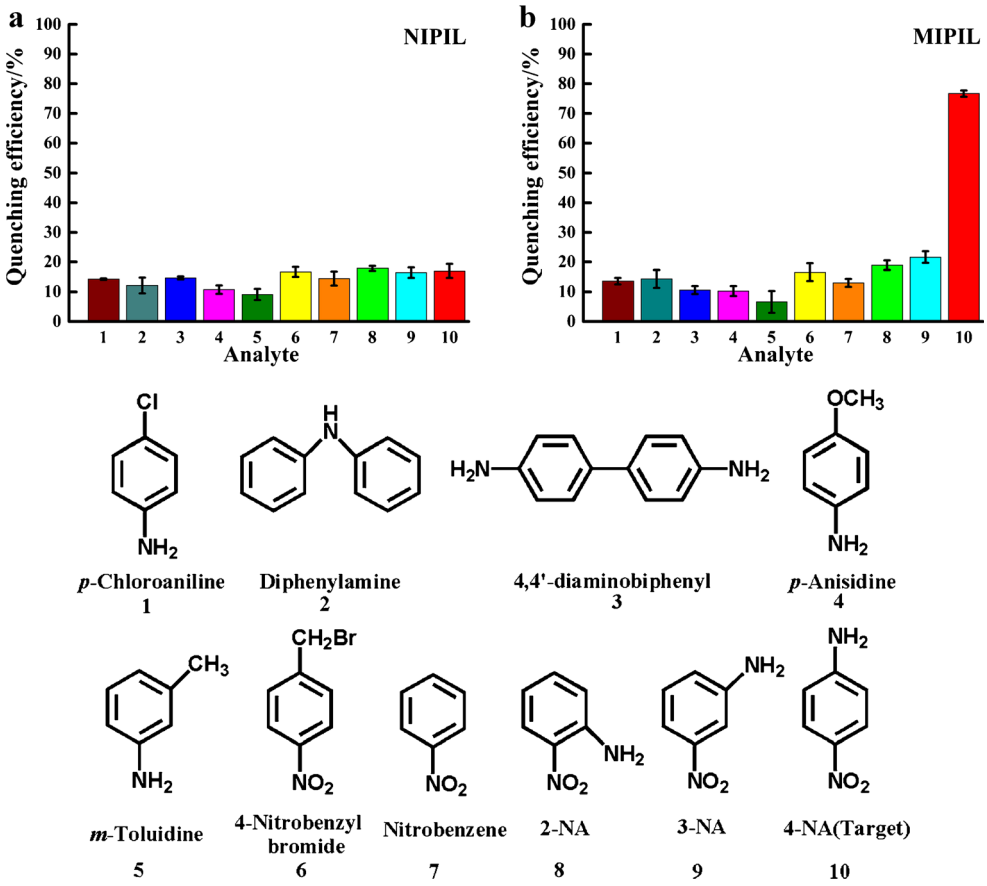

Fig. 4 (**a**, **b**) Fluorescence quenching efficiency of NIPIL and MIPIL sensors with the addition of different aromatic compounds (1 μM)

Table 2 Detection and recovery of 4-NA in actual water samples ($n = 6$)

Sample	Added 4-NA (nM)	Found 4-NA (nM)	Recovery (%)	RSD (%)
Canal water	2.67	2.73	102.4	4.58
	30.0	28.3	97.7	2.55
	50.0	51.6	103.2	4.36
	100.0	99.3	99.3	3.82

(4) *p*-anisidine, (5) *m*-toluidine, (6) 4-nitrobenzyl bromide, (7) nitrobenzene, (8) 2-NA, and (9) 3-NA. As shown in Fig. 4, the quenching effect of 4-NA and its analogs on the NIPIL sensor was similar, but 4-NA exerted a significantly higher quenching effect on the MIPIL sensor than on its analogs. Although 2-NA and 3-NA had a similar structure as the template molecule 4-NA, the degree of fluorescence quenching on the MIPIL sensor was less than that of 4-NA. The results showed that the MIPIL sensor had a good selectivity for 4-NA, which was much higher than that of the NIPIL sensor.

Measurements of real water and industrial wastewater samples

The constructed MIPIL fluorescence sensor was utilized for 4-NA detection in the actual water samples, which were obtained from Beijing–Hangzhou Grand Canal in Jiaxing City. The suspended impurities in the real water samples were removed using a 0.45-μm filter before detection, and then the actual water samples were directly used for detection. During the measurement of the actual water samples, we found that the water samples did not respond to the MIPIL fluorescence sensor. Therefore, we used the method of adding different concentrations of 4-NA to the real water samples for recovery investigation. Four different concentrations (2.67, 30, 50, and 100 nM) were selected for spike recovery, and the results are shown in Table 2. The recoveries were 97.7–103.2%. These values reveal the high accuracy of the proposed assay.

In order to further evaluate the practicability and accuracy of the proposed MIPIL fluorescent sensor, we used the sensor to detect the content of 4-NA in industrial wastewater and spiked industrial wastewater, and compared it with the method of HPLC. At first, we tested the standard water samples containing 4-NA by Agilent 1260 HPLC and established HPLC method. The linear equation was $Y = 3.136C_{4\text{-NA}} - 15.396$, in which Y was the peak area and the correlation coefficient was 0.995. It can be seen from Fig. 5a and b that there is a good linear relationship between peak area and concentration in the concentration range of 10–1000 μM. Next, the proposed MIPIL fluorescent sensor and HPLC method were used to detect the content of 4-NA in industrial wastewater samples, and their detection results were compared. It can be seen from Fig. 5c and d that the detection results of the two methods are consistent. It means that the proposed method may be applied to the rapid and accurate detection of 4-NA in industrial wastewater.

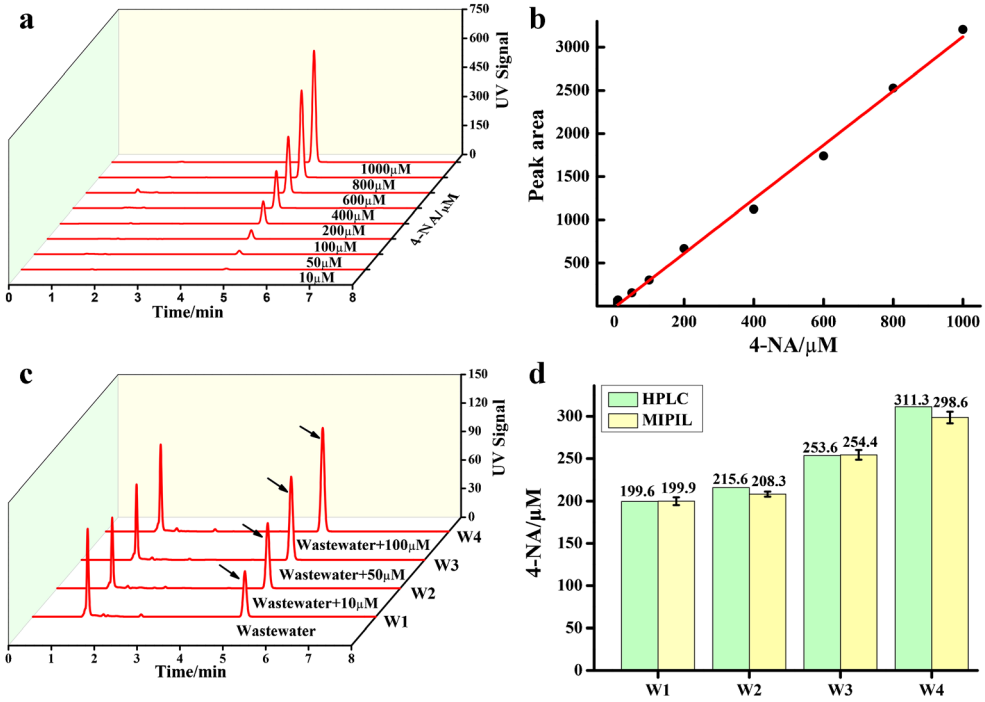

Fig. 5 (**a**) Detection of different concentrations of 4-NA using the method of HPLC. (**b**) The standard curve of the method of HPLC. (**c**) Determination of 4-NA in industrial wastewater and spiked industrial wastewater using the method of HPLC. (**d**) Comparison of detection results of 4-NA in industrial wastewater and spiked industrial wastewater by the method of HPLC and MIPIL fluorescent sensor

Conclusions

In short, 4-bromomethyl-7-methoxycoumarin as a fluorophore was applied to the preparation of a new ILFM, and a novel MIPIL fluorescence sensor was successfully developed for the detection of 4-NA. The sensor has the advantages of low cost, easy preparation, simple operation, rapid detection, and high specificity and sensitivity to 4-NA. Given that the sensor has good test performance, it has a potential application value in the immediate detection of 4-NA in industrial wastewater and environmental water.

Funding information This research is supported by the National Natural Science Foundation of China (Nos. 21677060 and 51503079), the Public Welfare Technology Research Project of Zhejiang Province (Nos. LGF18B050004 and LGC19B050007), the Natural Science Foundation of Zhejiang Province (No. LY20B050009), and the Science and Technology Plan Project of Jiaxing City, China (Nos. 2017AY33034 and 2018AY11002).

Compliance with ethical standards Industrial wastewater was provided by a chemical factory in Jiangsu Province (China), and it was authorized by the chemical factory to be used for the study.

Conflict of interest The authors declare that they have no conflict of interest.

References

1. Benigni R, Passerini L. Carcinogenicity of the aromatic amines: from structure–activity relationships to mechanisms of action and risk assessment. Mutat Res. 2002;511(3):191–206.
2. Ahmad R, Tripathy N, Ahn MS, Hahn YB. Development of highly-stable binder-free chemical sensor electrodes for p-nitroaniline detection. J Colloid Interface Sci. 2017;494:300–6.
3. Zheng K, Zhang T, Lin P, Han Y, Li H, Ji R, et al. 4-Nitroaniline degradation by TiO_2 catalyst doping with manganese. J Chem. 2015:1–6.
4. Niazi A, Ghasemi J, Yazdanipour A. Simultaneous spectrophotometric determination of nitroaniline isomers after cloud point extraction by using least-squares support vector machines. Spectrochim Acta A. 2007;68(3):523–30.
5. Hasani M, Emami F. Evaluation of feed-forward back propagation and radial basis function neural networks in simultaneous kinetic spectrophotometric determination of nitroaniline isomers. Talanta. 2008;75(1):116–26.
6. Wang M, De Vivo B, Lu W, Muniz-Miranda M. Sensitive surface-enhanced Raman scattering (SERS) detection of nitroaromatic pollutants in water. Appl Spectrosc. 2014;68(7):784–8.
7. Zhang Y, Su K, Ha Y, Chen S, Chen W, Sun C, et al. Silver molecularly imprinting polymer for the determination of p-nitroaniline by surface enhanced Raman scattering. Anal Lett. 2019;52(12):1888–99.
8. Laghrib F, Farahi A, Bakasse M, Lahrich S, El Mhammedi MA. Chemical synthesis of nanosilver on chitosan and electroanalysis activity against the p-nitroaniline reduction. J Electroanal Chem. 2019;845:111–8.
9. Bakhsh EM, Ali F, Khan SB, Marwani HM, Danish EY, Asiri AM. Copper nanoparticles embedded chitosan for efficient detection and reduction of nitroaniline. Int J Biol Macromol. 2019;131:666–75.
10. Laghrib F, Farahi A, Bakasse M, Lahrich S, El Mhammedi MA. Voltammetric determination of nitro compound 4-nitroaniline in aqueous medium at chitosan gelified modified carbon paste electrode (CS@CPE). Int J Biol Macromol. 2019;131:1155–61.
11. Qian L, Hong H, Han M, Xu C, Wang S, Guo Z, et al. A ketone-functionalized carbazolic porous organic framework for sensitive fluorometric determination of p-nitroaniline. Microchim Acta. 2019;186(7):457.
12. Cao Y, Wang S, Wu W, Peng H, Yu Y, Zhu D. Cucurbit[6]uril modified CdTe quantum dots fluorescent probe and its selective analysis of p-nitroaniline in environmental samples. Talanta. 2019;199:667–73.
13. Tong C, Guo Y, Liu W. Simultaneous determination of five nitroaniline and dinitroaniline isomers in wastewaters by solid-phase extraction and high-performance liquid chromatography with ultraviolet detection. Chemosphere. 2010;81(3):430–5.
14. Xiao P, Bao C, Jia Q, Su R, Zhou W, Jia J. Determination of nitroanilines in hair dye using polymer monolith microextraction coupled with HPLC. J Sep Sci. 2011;34(6):675–80.
15. Zhao S, Ding J-G, Zheng T-R, Li K, Li B-L, Wu B. The 3D and 2D cadmium coordination polymers as luminescent sensors for detection of nitroaromatics. J Lumin. 2017;188:356–64.
16. Wu P, Liu Y, Li Y, Jiang M, Li X-l, Shi Y, et al. A cadmium(ii)-based metal–organic framework for selective trace detection of nitroaniline isomers and photocatalytic degradation of methylene blue in neutral aqueous solution. J Mater Chem A. 2016;4(42):16349–55.
17. Guo X, Lv J, Zhang W, Wang Q, He P, Fang Y. Separation and determination of nitroaniline isomers by capillary zone electrophoresis with amperometric detection. Talanta. 2006;69(1):121–5.
18. Sanchis Y, Coscolla C, Yusa V. Comprehensive analysis of photoinitiators and primary aromatic amines in food contact materials using liquid chromatography high-resolution mass spectrometry. Talanta. 2019;191:109–18.
19. Luongo G, Iadaresta F, Moccia E, Ostman C, Crescenzi C. Determination of aniline and quinoline compounds in textiles. J Chromatogr A. 2016;1471:11–8.
20. Kampfer P, Crettaz S, Nussbaumer S, Scherer M, Krepich S, Deflorin O. Quantitative determination of 58 aromatic amines and positional isomers in textiles by high-performance liquid chromatography with electrospray ionization tandem mass spectrometry. J Chromatogr A. 2019;1592:71–81.
21. Tolgyesi A, Sharma VK. Quantification of aromatic amines derived from azo colorants in textile by ion-pairing liquid chromatography tandem mass spectrometry. J Chromatogr B. 2020;1137:121957.
22. The Huy B, Seo MH, Zhang X, Lee YI. Selective optosensing of clenbuterol and melamine using molecularly imprinted polymer-capped CdTe quantum dots. Biosens Bioelectron. 2014;57:310–6.
23. Liu G, Huang X, Li L, Xu X, Zhang Y, Lv J, et al. Recent advances and perspectives of molecularly imprinted polymer-based fluorescent sensors in food and environment analysis. Nanomaterials (Basel). 2019;9(7):1030.
24. Hallett JP, Welton T. Room-temperature ionic liquids: solvents for synthesis and catalysis. 2. Chem Rev. 2011;111(5):3508–76.
25. Sing KS. Reporting physisorption data for gas/solid systems with special reference to the determination of surface area and porosity (recommendations 1984). Pure Appl Chem. 1985;57(4):603–19.
26. Li B, Huang X, Liang L, Tan B. Synthesis of uniform microporous polymer nanoparticles and their applications for hydrogen storage. J Mater Chem. 2010;20(35):7444–50.
27. Zhu X, Yu J, Jiang C, Cheng B. Enhanced room-temperature HCHO decomposition activity of highly-dispersed Pt/Al_2O_3 hierarchical microspheres with exposed {110} facets. J Ind Eng Chem. 2017;45:197–205 2015.
28. Laghrib F, Ajermoun N, Hrioua A, Lahrich S, Farahi A, El Haimouti A, et al. Investigation of voltammetric behavior of 4-

nitroaniline based on electrodeposition of silver particles onto graphite electrode. Ionics. 2018;25(6):2813–21.
29. Wei F, Cai X, Nie J, Wang F, Lu C, Yang G, et al. A 1,2,3-triazolyl based conjugated microporous polymer for sensitive detection of p-nitroaniline and Au nanoparticle immobilization. Polym Chem. 2018;9(27):3832–9.
30. Lu X, Yang Y, Zeng Y, Li L, Wu X. Rapid and reliable determination of p-nitroaniline in wastewater by molecularly imprinted fluorescent polymeric ionic liquid microspheres. Biosens Bioelectron. 2018;99:47–55.
31. Ji NN, Shi ZQ, Hu HL, Zheng HG. A triphenylamine-functionalized luminescent sensor for efficient p-nitroaniline detection. Dalton Trans. 2018;47(21):7222–8.
32. Chakraborty G, Das P, Mandal SK. Strategic construction of highly stable metal-organic frameworks combining both semi-rigid tetrapodal and rigid ditopic linkers: selective and ultrafast sensing of 4-nitroaniline in water. ACS Appl Mater Interfaces. 2018;10(49):42406–16.
33. Shu T, Wang N, Li Y, Fu D, Fan H, Luo M, et al. A new three-dimensional Cd(II) metal-organic framework for highly selective sensing of Fe^{3+} as well as nitroaromatic compounds. ChemistrySelect. 2017;2(36):12046–50.
34. Laghrib F, Boumya W, Lahrich S, Farahi A, El Haimouti A, El Mhammedi MA. Electrochemical evaluation of catalytic effect of silver in reducing 4-nitroaniline: analytical application. J Electroanal Chem. 2017;807:82–7.